Int J Cardiovasc Imaging (2017) 33:83–95
DOI 10.1007/s10554-016-0980-3

ORIGINAL PAPER

Left ventricular non-compaction and idiopathic dilated cardiomyopathy: the significant diagnostic value of longitudinal strain

Fanny Tarando[1,6] · Damien Coisne[2,6] · Elena Galli[1,3,6] · Chloé Rousseau[4,6] · Frédéric Viera[2,6] · Christian Bosseau[1,6] · Gilbert Habib[5,6] · Mathieu Lederlin[5,6] · Frédéric Schnell[3,6,7] · Erwan Donal[1,3,6]

Received: 3 August 2016 / Accepted: 16 September 2016 / Published online: 22 September 2016

Abstract Left ventricular non-compaction (LV NC) is characterized by abnormal trabeculations that are mainly at the LV apex. Distinction between LV NC and non-specific dilated cardiomyopathies (DCMs) remains often challenging. We sought to find additive tools comparing the longitudinal strain characteristics of LVNC versus idiopathic DCM in a cohort of patients. 48 cases of LVNC (derivation cohort) were compared with 45 cases of DCM. Global and regional multi-layer (sub-endocardial, mid-wall, and sub-epicardial) LV longitudinal strain analysis was performed. Results were compared to define the best tool for distinguishing LVNC from DCM. A validation cohort (41 LVNC patients) was then used to assess the performance of the proposed diagnostic tools. In the derivation cohort, longitudinal deformation (strain) was greater in LVNC than in DCM patients. Longitudinal shortening was greater in the non-compacted segments than in the compacted ones. A mid-wall strain base-apex gradient had 88.4% sensitivity and 66.7% specificity in distinguishing LVNC from DCM (AUC = 0.83; cut-off of −23 or |0.23|%). In a multivariable model, the base-apex mid-wall gradient in an apical 4-chamber view was the only independent echocardiographic criteria (OR = 0.76, CI 95% [0.66; 0.90], p = 0.0010) allowing the distinction between LVNC and DCM. In the validation cohort, the base-apex mid-wall gradient of strain had 88.4% sensitivity, 85.7% negative predictive values for the diagnosis of LVNC. Longitudinal strain, especially the base-apex longitudinal gradient of strain, appears as an additive valuable tool for distinguishing LVNC from DCM.

Keywords Left ventricular non-compaction · Echocardiography · Longitudinal strain · Dilated cardiomyopathy

Abbreviations

LVNC	Left ventricular non-compaction
CMR	Cardiac magnetic resonance imaging
DCM	Dilated cardiomyopathy
GLS	Global longitudinal strain
AUC	Area under the curve
LV	Left ventricle
TDI	Tissue doppler imaging
TAPSE	Tricuspid annular plane systolic excursion

Introduction

Left ventricular non-compaction (LVNC) is a cardiomyopathy characterized by prominent trabeculations associated with deep, inter-trabecular recesses that communicate with the ventricular cavity [1]. The distinction between non-specific dilated cardiomyopathy (DCM) and LVNC is debated, as is the pathophysiology and genetic determinants

✉ Erwan Donal
erwan.donal@chu-rennes.fr

1 Service de Cardiologie and CIC-IT 1414, Hôpital Pontchaillou - CHU Rennes, 2 rue Henri Le Guillou, 35000 Rennes, France

2 Service de Cardiologie, CHU Poitiers, Poitiers, France

3 LTSI, INSERM 1099, Université Rennes-1, Rennes, France

4 CIC-P 1414, CHU Rennes, Rennes, France

5 Service de Cardiologie, CHU Marseille, Marseille, France

6 Service d'Imagerie médicale, CHU Rennes, Rennes, France

7 Médecine du Sport et Service de Physiologie, CHU Rennes, Rennes, France

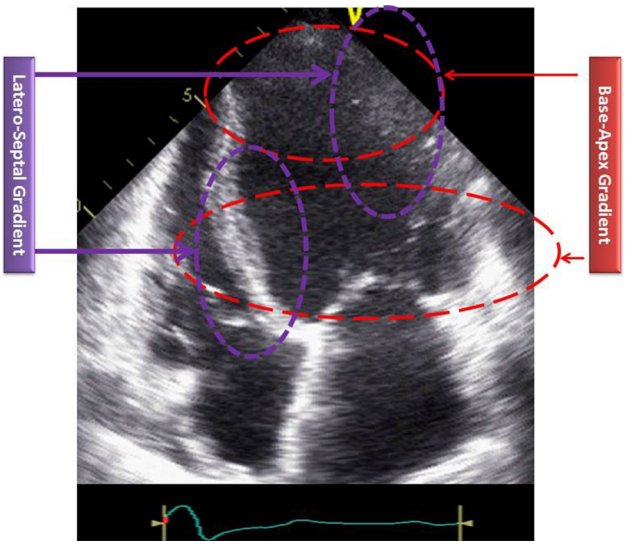

Fig. 1 Example of an apical 4-chamber view of a DCM with the definition of latero-septal segments and basal–apical ones that were used for defining the gradients

of these diseases [2–4]. In a recent study, the application of pre-defined criteria for the diagnosis of LVNC was associated with a significant inter-observer disagreement in 35 % of cases [5–7].

Transthoracic echocardiography and cardiac magnetic resonance imaging (CMR) are often used in combination for the diagnosis of LVNC, in order to circumvent the absence of an irrefutable test provided by either approach alone. Several echocardiographic definitions [1, 3, 8, 9] and at least two CMR definitions [10, 11] have been published. These definitions were tested on limited numbers of patients, with no systematic confrontation with the pathology. Applying all of these criteria can lead to excess in diagnosis and contradictory results [1, 12–14].

Trabeculations are not specific, since they can be found in the DCM, which can make differential diagnosis from LVNC difficult [15]. Therefore, some authors have suggested imaging deformation as a possible diagnostic support tool when diagnosis is difficult [16, 17].

The aim of the present study was to evaluate multilayer longitudinal strain in patients with LVNC and non-ischemic DCM in order to define additional echocardiographic criteria for the differentiation of these two disease entities. The reliability of our results was then tested in a validation cohort composed of LVNC patients enrolled in another center.

Methods

Population

The study population was composed of 45 non-ischemic DCM patients and 48 LVNC (derivation cohort) patients who were enrolled prospectively at the University Hospital of Rennes between 2009 and 2014. The population was completed with a validation cohort, composed of 41 LVNC patients enrolled in the same period at the University Hospital of Poitiers and. The exclusion criteria were: age <18 years, coronary artery disease (every patient had a coronary-CT or

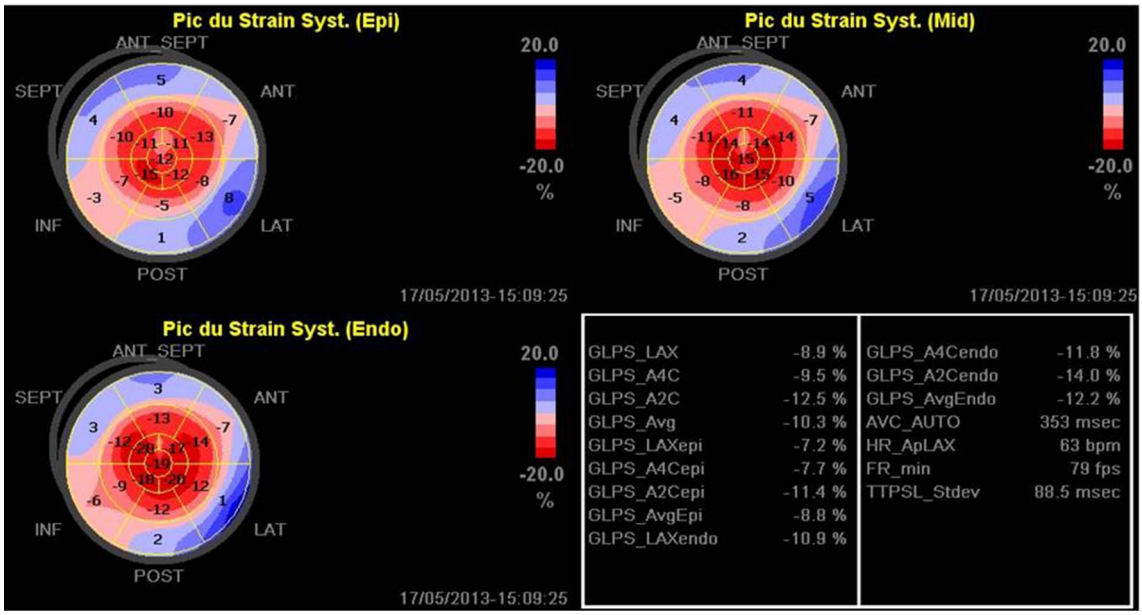

Fig. 2 Bull eyes of the longitudinal strains recorded in the three myocardial layers in a patient with a LVNC. The apex-base gradient in longitudinal deformation is striking

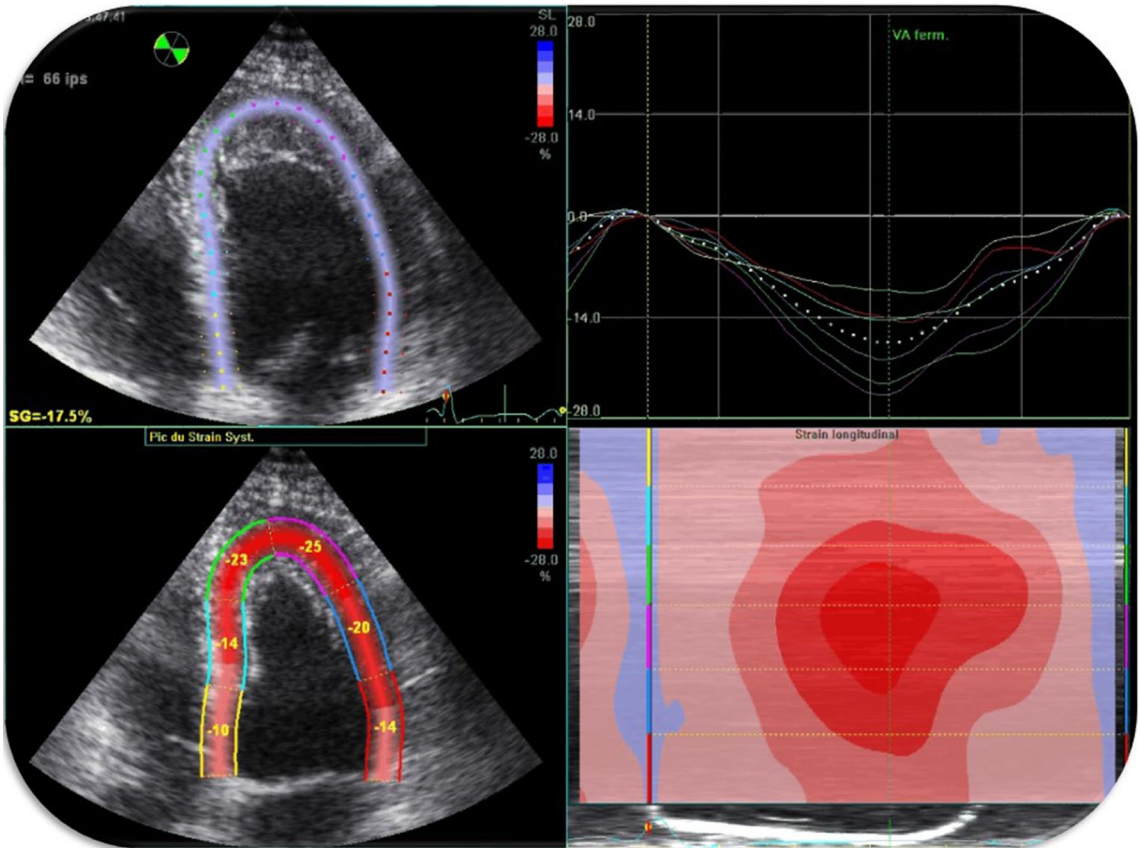

Fig. 3 Example of the tracing of the region of interest for the calculation of longitudinal strain. Example of it was dealt with the deep trabeculations

angiography), more than moderate concomitant valve disease, congenital cardiomyopathy, hemodynamic instability, recent (<1 months) hospitalization for cardiac decompensation, uncontrolled arrhythmias, unsuitable acoustic window (n = 0 in this cohort requiring a cardiac magnetic resonance and an echocardiography for affirming the diagnosis of LVNC and DCM). For patients with LVNC the diagnostic suspicion was formulated by echocardiography according to the Jenny criteria and confirmed by CMR [1, 10]. The diagnosis of LVNC by CMR was retained if non-compacted to compacted myocardium ratio in end-diastole was >2.3 (Petersen's criteria) or if the non-compacted mass exceeded 20 % of the total cardiac mass (Jacquier's criteria) [11]. The diagnosis of LVNC was based on the analysis of the echocardiographic and CMR data by at least two independent experts. An agreement between these two was mandatory for affirming the diagnosis of LVNC. The diagnosis of DCM was formulated according to the recommendations of the Working Group on Myocardial and Pericardial Diseases of the European Society of Cardiology [18].

The study was conducted in accordance with the "Good Clinical Practice" Guidelines, as stated in the Declaration of Helsinki. The study was reviewed by the independent ethics committees of all of the participating centers. All of the patients gave their written, informed consent (ethic committee authorization 35RC14-9767).

Clinical and biological data

Clinical data including age, gender, the New York Heart Association (NYHA) functional class, concomitant cardiovascular risk factors (hypertension, hypercholesterolemia, diabetes), and therapy were collected for each patient. Standard biological results and NT-proBNP (N terminal- pro brain natriuretic peptide) were also reported. A 12- lead electrocardiography was registered for each patient and data regarding, HR, PR and QRS duration, repolarization abnormalities were reported.

2D-Echocardiography

Transthoracic echocardiography was performed at rest on a Vivid 7 or Vivid E9 ultrasound system (GE Healthcare, Horten, Norway) and images were recorded on a remote station and analyzed using a dedicated software (EchoPAC PC version BT 13, GE Heathcare, Horten, Norway) [19]. LV linear dimensions, volumes, LV ejection fraction (LV EF), left and right atrial volumes were calculated as recommended

Table 1 Characteristics of the derivation cohort

Variable	LVNC	DCM	p
Male sex	29 (60%)	33 (73%)	0.1867 (K)
Age (years)	50 ± 17	66 ± 9	<0.0001 (S)
Body mass index (Kg/m^2)	24.8 ± 4.5	26.7 ± 4.4	0.0527 (S)
Pacemaker	0	3 (6.7%)	0.3249 (F)
ICD	4 (9.1%)	3 (6.7%)	
CRT	1 (2.3%)	0	
Diabetes	5 (10.6%)	6 (13.3%)	0.6904 (K)
Smokers	14 (29.8%)	18 (40.0%)	0.3039 (K)
Hypercholesterolemia	16 (34.0%)	24 (53.3%)	0.0621 (K)
Arterial hypertension	21 (44.7%)	14 (31.1%)	0.1802 (K)
Kidney failure (creatinine clearance ≤ 60 mL/min)	7 (15.6%)	15 (34.1%)	0.0427 (K)
NYHA class			
I	18 (38.3%)	0	
II	18 (38.3%)	13 (28.9%)	
III	11 (23.4%)	32 (71.1%)	<0.0001 (F)
Treatment			
ACE	31 (67.4%)	42 (95.5%)	0.0007 (K)
Beta blockers	30 (65.2%)	43 (97.7%)	<0.0001 (K)
Aldosterone antagonists	12 (26.1%)	15 (34.1%)	0.4075 (K)
Diuretics	11 (23.9%)	41 (93.2%)	<0.0001 (K)

BMI body mass index, *NYHA* New York Heart Association, *ACE-inhibitor* angiotensin-converting enzyme, *LBBB* left bundle branch block

Qualitative parameters: χ^2 (=K) or Fisher (=F) tests

Quantitative parameters: Mean ± standard deviation, Student (S) or Wilcoxon (W) tests

Table 2 Echocardiographic measurements in the derivation cohort

Variable	LVNC	DCM	p
IVSd (mm)	8.8 ± 2.4	7.6 ± 1.6	0.0636 (W)
LVESD (mm)	32.2 ± 6.7	36.7 ± 5.0	0.0006 (S)
PWd (mm)	8.6 ± 2.4	8.4 ± 1.4	0.9776 (W)
LVEDD (mm)	49.0 ± 12.7	57.6 ± 9.1	0.0004 (S)
LA volume (mL/m²)	32.2 ± 13.0	49.7 ± 19.2	<0.0001 (S)
LVEDV (mL)	167.0 ± 81.3	235.1 ± 67.3	<0.0001 (S)
LVESV (mL)	108.1 ± 75.0	168.8 ± 53.3	<0.0001 (S)
LVEF (%)	39.6 ± 13.1	27.9 ± 5.1	<0.0001 (S)
Cardiac Index (mL/min/m²)	2.4 ± 0.8	2.1 ± 1	0.2512 (S)
Mitral regurgitation (1–3/4)	0.6 ± 0.9	1.5 ± 0.8	<0.0001 (S)
E/A	1.1 ± 0.7	1.3 ± 0.8	0.4100 (S)
E-DT (ms)	196.7 ± 68.5	171.1 ± 67.4	0.0788 (S)
E/e′ (cm/s)	11.6 ± 7.8	14.6 ± 6.3	0.0596 (S)
RA area (cm²)	14.1 ± 3.5	16.4 ± 4	0.0220 (W)
RV-FR(%)	0.33 ± 0.13	0.41 ± 0.15	0.0798 (S)
TAPSE (mm)	22.4 ± 4.9	17.9 ± 3.4	<0.0001 (S)
RV-s′ (cm/s)	11.9 ± 2.7	10.9 ± 2.7	0.1247 (S)
RV-2D strain (%)	−15.6 ± 4.8	−19.7 ± 6.6	0.0033 (S)
SPAP (mmHg)	31.8 ± 11.0	34.2 ± 10.3	0.3301 (W)

dIVS diastolic interventricular septum thickness in diastole, *LVEDD* left ventricular end-diastolic diameter, *dPW* diastolic posterior wall, *LVESD* LV end-systolic diameter, *LA* left atrial, *LVEDV* LV end-diastolic volume, *LVESV* LV end-systolic volume, *LVEF* LV ejection fraction, *E-DT* mitral inflow E-wave deceleration time, *RVFR* right ventricular fractional area changes, *SPAP* systolic pulmonary arterial pressure

Qualitative parameters: χ^2 test (K)

Quantitative parameters: mean ± standard deviation, Student (S) ou Wilcoxon (W) tests

[20]. TDI was used to detect the lateral and septal mitral annulus velocities and the average value estimated mitral e′ (Figs. 1, 2).

Analysis of LV longitudinal deformations was conducted for each patient using the loops from the apical 4-, 3- and 2-chamber views. According to the regional thickness of each segment the region of interest was adapted to systematically include the endocardial and the epicardial borders. The regional adaptation of the size of the region of interest was possible on the EchoPAC version we were using (EchoPAC B13, GE Healthcare, Horten, Norway). The borders of the region of interests were limited to region were some myocardium was seen. In case of very deep recesses, particularly in the apex, the strain was measured staying not too fat from the epicardium (Fig. 3) A semi-automatic analysis of the endocardial and epicardial contours was then carried out to determine the global and regional longitudinal deformations in the sub-endocardial, mid-wall and sub-epicardial layers.

For each myocardial segment, the maximum value of the amplitude peaks of strain and the value of the global longitudinal strain of each layer were recorded (Figs. 1, 2).

For each myocardial layer, we compared the longitudinal strain values obtained in basal and apical segments and in the septal and antero-laterall segments (Fig. 1) in order to define the base-apex and latero-septal gradients. All the speckle tracking analysis were done offline and by an investigator blinded to the final diagnostic of each patient included in the analysis.

Statistical analyses

Quantitative variables are described as means ± standard deviation and compared using the Student's t-test or the Wilcoxon's test as appropriate. Qualitative variables are presented as number and percentage (%) and compared χ^2 tests or Fisher's exact tests.

For analysis of quantitative data collected from the same patient (paired data), paired Student's t-test was used.

Table 3 Longitudinal strain: global and multi-layers in the derivation cohort

Variable	LVNC	DCM	p
Global longitudinal Strain EPI	−10.6 ± 4.4	−6.4 ± 2.3	<0.0001 (S)
Global longitudinal Strain MID (=GLS)	−12.2 ± 5	−7.4 ± 2.4	<0.0001 (S)
Global longitudinal Strain ENDO	−14.2 ± 5.6	−8.7 ± 2.6	<0.0001 (S)

EPI subepicardial myocardial layers, *MID* mid-layers, *ENDO* sub-endocardial layers

ROC curves were used to define the apex-base and septo-lateral cut-offs able to identify LV NC.

The area under the curve (AUC) that differentiates LVNC from DCM was defined for each parameter or combination of parameters, and the AUC values were compared.

The threshold was chosen based on the maximum sensitivity and specificity (Youden index). The AUC values were compared using the nonparametric method proposed by DeLong et al. [21]. Clinically relevant variables that were significant (<0.05) were tested via multivariate logistic regression; model selection was performed rather than step-down regression.

Results

The general characteristics of the studied population are described in Table 1. With respect to LVNC, DCM patients were older and more often symptomatic (dyspnea). Echocardiography data are depicted in Table 2. DCM patients had higher LA and LV volumes, lower LVEF and impaired right ventricular performance with respect to LVNC (Table2).

Myocardial deformations

The absolute value of global, epicardial, mid-wall, and sub-endocardial strain was significantly higher in LVNC that in DCM (Table 3). As shown in Table 4, in the LVNC group epicardial, endocardial, and mid-wall strains were significantly higher in the antero-lateral wall than in the septum. In DCM, a significant difference between the lateral and septal strain was observe in endocardial strain only.

Interestingly, in LVNC, basal strain was significantly lower than apical strain in all LV layers, which is in opposition with what can be observed in DCM.

As shown in Fig. 1, the deformations at the base were lower than those at the apex of the LV (Table 4).

Latero-septal and base-apex gradients

Only the sub-endocardial latero-septal gradient differentiated LVNC from DCM (Fig. 2), Table 5.

In opposite, all the base to apex gradient were significantly and more convincingly different between LVNC and DCM. (Table 5).

ROC curve analysis

In order to define the gradient that best discriminates LVNC from DCM, ROC curves were calculated for each base-to-apex and septal-to-lateral gradient (Fig. 4). The optimal AUC values were obtained using the global base-apex gradient in the mid-wall (AUC = 0.83), retaining a threshold of −23 (or |0.23|), a sensitivity of 88.4% and a specificity of 66.7% (PPV = 71.7%, NPV = 85.7%). The sub-endocardial base-apex gradient in apical 4-chamber view was characterized by an AUC = 0.824, with a threshold of −1 (or |1|), a sensitivity of 81.4% and a specificity of 66.7% (PPV

Table 4 Myocardial strains in compacted versus non-compacted regions

	LVNC			DCM		
Variable	Antero-lateral	Septum	p	Antero-lateral	Septum	*p*
Strain EPI	−10 ± 6	−8.1 ± 6.9	0.0053	−6 ± 3.3	−5.2 ± 4.2	0.3132
MID	−11.9 ± 7.1	−9.1 ± 7.1	<0.0001	−7.2 ± 3.7	−5.7 ± 4.3	0.0927
ENDO	−15.2 ± 8.8	−10.3 ± 7.5	<0.0001	−8.9 ± 4.6	−6.4 ± 4.5	0.0182
	Base	Apex		Base	Apex	
4ch EPI	−9.2 ± 6.4	−11.4 ± 5.2	p = 0.0170	−8.7 ± 6.2	−5.2 ± 3.1	*p* = 0.0006
4ch MID	−10.1 ± 6.5	−14 ± 6.7	p = 0.0005	−9.9 ± 6.9	−6.6 ± 3.6	*p* = 0.0040
4ch ENDO	−11.1 ± 6.6	−18.7 ± 8.5	p < 0.0001	−11.2 ± 7.6	−8.7 ± 4.6	*p* = 0.0473
bull eyes EPI	−9.4 ± 5	−11.5 ± 5.3	p = 0.0007	−7.2 ± 2.6	−5.3 ± 2.9	*p* = 0.0009
bull eyes MID	−10.2 ± 5.3	−14.2 ± 6.5	p < 0.0001	−8 ± 2.8	−6.6 ± 3.4	*p* = 0.0185
bull eyes ENDO	−11 ± 5.5	−18.5 ± 8.7	p < 0.0001	−9 ± 3.1	−8.5 ± 4.3	*p* = 0.4294

Abreviations are the one from previous tables & 4ch: 4 chamber apical view

Table 5 Comparison of the myocardial strain gradients between LVNC and DCM in the derivation cohort

Variable	LVNC	DCM	p
Latero-septal gradient EPI	−1.8 ± 4.3	−0.8 ± 5.2	0.3001 (S)
Latero-septal gradient MID	−2.8 ± 4.1	−1.4 ± 5.8	0.2132 (S)
Latero-septal gradient ENDO	−4.9 ± 4.2	−2.4 ± 6.7	0.0322 (S)
Base-apex Gradient 4-chamber EPI	−2.2 ± 5.8	−3.5 ± 6.4	<0.0001 (S)
Base-apex Gradient 4-chamber MID	−3.8 ± 6.6	−3.3 ± 7.2	0.0001 (S)
Base-apex Gradient 4-chamber ENDO	−7.6 ± 7.3	−2.5 ± 8.2	<0.0001 (S)
Base-apex Gradient global EPI	−2.0 ± 3.6	−1.8 ± 3.4	<0.0001 (S)
Base-apex Gradient global MID	−3.9 ± 4.2	−1.4 ± 3.9	<0.0001 (S)
Base-apex Gradient global ENDO	−7.5 ± 5.8	−0.5 ± 4.7	<0.0001 (S)

Abbreviations are the one from previous tables

(positive predictive value) = 70 % NPV (negative predictive value) = 78.9 %). Table 6 shows the comparison of AUC values.

Multivariate analysis

The mid-wall base apex gradient was an independent echocardiographic parameter able to distinguish DCM and LVNV (Table 6).

Application of the results obtained from the derivation cohort to an independent validation cohort

A comparison of the characteristics of the validation and derivation cohorts is presented in Appendix The base-apex gradients that were informative in the derivation cohort (cut-offs defined by the ROC-analysis) were tested in the validation cohort. For the base-apex gradient, using the strain recorded in the mid-wall and considering the cut-off of −0.23 that was defined in the derivation cohort, the sensitivity for LVNC diagnosis was 80.5 % [65.1 %; 91.2 %], the specificity was 35.7 % [21.6 %; 52.0 %], the positive predictive value was 55.0 % [41.6 %; 67.9 %], and the negative predictive value was 65.2 % [42.7 %; 83.6 %].

Discussion

LVNC diagnosis remains challenging [4]. Kohli et al. [14] demonstrated the excessive sensitivity of the currently selected morphological criteria. Using echocardiography and CMR data, diagnosis is based on a consensus among experts [15]. Our study provides relevant elements for distinguishing LVNC and DCM based not on anatomy but on myocardial deformation parameters.

Values of strain imaging

Echocardiographic techniques, such as tissue Doppler imaging and speckle tracking, can help to identify and to stratify the risk of cardiomyopathies [22]. It might allow the clinician to distinguish regional myocardial abnormalities [23], such as those in the trabeculated segments in LVNC patients. Previous authors have suggested that deformation imaging could help to differentiate LVNC from DCM [14, 15]. Because in LVNC, trabeculations are commonly localized in the sub-endocardial layer, we examined multilayer longitudinal strain. We observed an "apical sparing" of longitudinal strain in non-compacted segments (sub-endocardial and in the mid-wall assessment of LV-regional strain in apical segments). The Longitudinal strain values in compacted segments were closed to the longitudinal strain regional values obtained in DCM-patients. Similar results were reported in a single-center series that did not distinguish sub-endocardial, sub-epicardial, and mid-wall longitudinal strains [16]. This result is confirming that LVNC is not a regional disease but a form of cardiomyopathy with abnormalities that are not focus on the non-compacted segments [24]. The Right ventricular function seems also being affected [25, 26] in a slightly different way in DCM and LVNC (more decrease in longitudinal strain). The Right ventricular involvement in LVNC has been, by the way, described previously [25, 27]. Patients carrying HCN4-695X and HCN4-P883R exhibit combined phenotypes: it has been reported biventricular hyper-trabeculation in multiple members of the families affected by the HCN4-695X mutation. Although LVEF was preserved and no overt structural abnormalities were initially noted [25, 26]. Our work is thus providing an additive approach for distinguishing the DCM from the LVNC. That is probably useful. The clinical course, the arrhythmogenic risk, the thombo-embolic risk and the genetic determinants might be different [28, 29]. There are no specific guidelines for LVNC treatment yet but the literature is underscoring that LVNC is a distinct for of cardiopathy [27, 28].

Gradients

Previous publications have demonstrated the value of longitudinal strain gradient ("apical sparing") for instance in the context of amyloidosis [23]. It has also been shown that the preferred location of LVNC is in the apical segments, primarily the inferior and antero-lateral walls [4]. The middle and basal segments of the septum are usually "compacted" [1, 8, 14]. To define the gradient with the threshold that yielded the

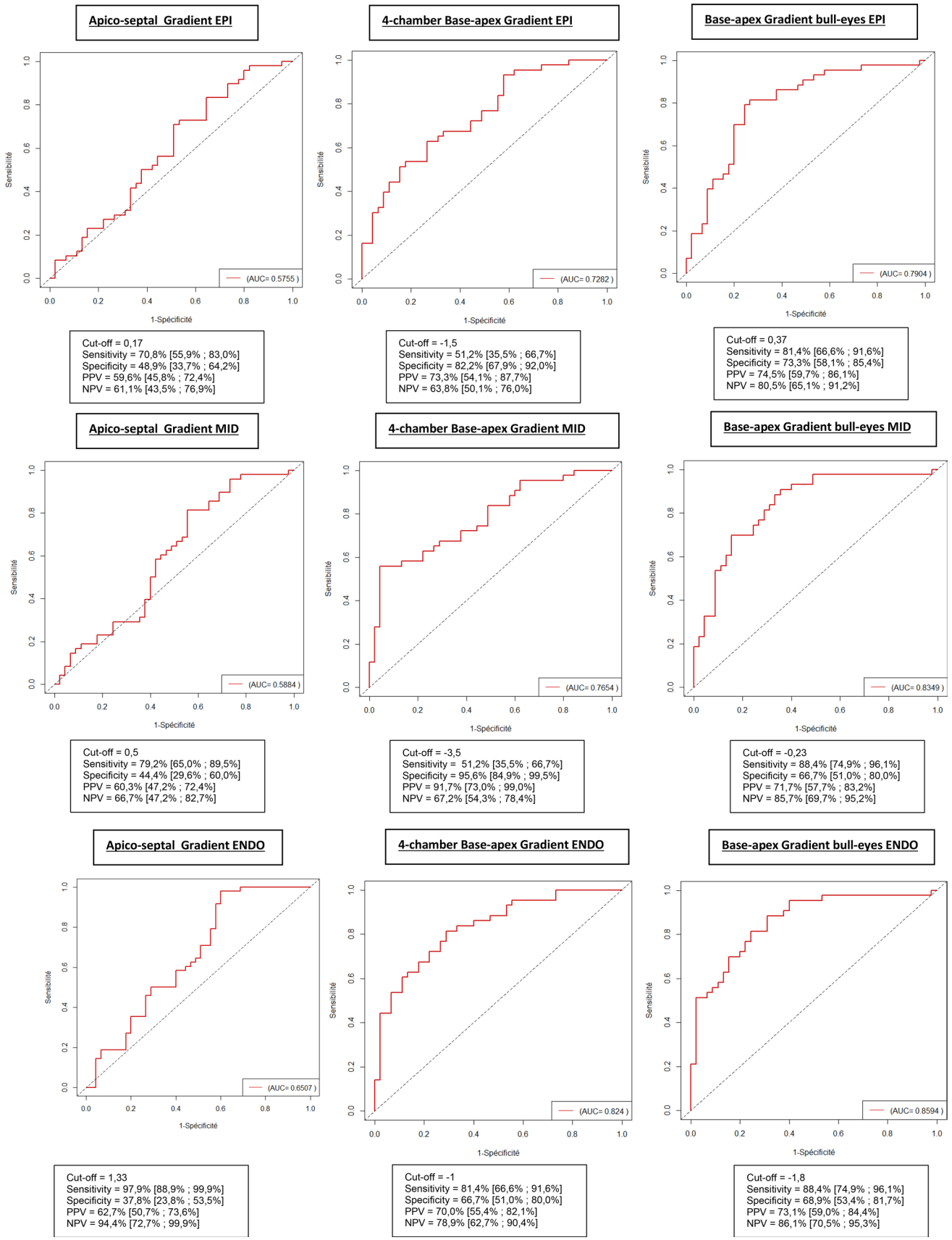

Fig. 4 ROC curves for strain parameters capability to distinguish DCM from LVNC

Table 6 Multivariable logistic regression using a backward step by step approach including: EPI base apex 4 chamber view, MID base apex 4 chamber view, ENDO base apex 4 chamber view, LVEDD, TAPSE, LVEDV, E/e′, EPI base apex bull-eyes, MID base-apex bull-eyes, ENDO base apex bull-eyes, age, LVEF

	Univariable analysis			Multivariable analysis (n = 87)	
VGNC (réf = DCM)	N	OR [IC95 %]	P-value	OR [IC95 %]	P-value
MID base apex	88	0.71 [0.61; 0.83]	<0.0001	0.76 [0.65; 0.90]	0.0010
Age	92	0.91 [0.87; 0.95]	<0.0001	0.93 [0.89; 0.97]	0.0019

most sensitivity and specificity in distinguishing LVNC, it was necessary to evaluate the areas with the most non-compaction segments (apex, apical and lateral walls) and those generally "compacted" (base and septum) such that the difference in strain between these walls would be most representative of the LVNC-cardiomyopathy. We therefore, analyzed different gradients: latero-septal and base-apex gradients, calculated from apical 4-chamber views and from the bull eyes (combining the 2D imaging data of 4-, 3- and 2-chamber apical views). No sub-epicardial gradient were relevant. In opposite, the mid-wall base/apex gradient (AUC = 0.835) of longitudinal strain, with a threshold of −0.23 (or |0.23|) % was observed as potentially valuable for distinguishing DCM and LVNC patients. The sub-endocardial gradient in apical 4-chamber view (AUC = 0.824) with a threshold of −1 % (or for simplifying|1|%) and the global base/apex sub-endocardial gradient (AUC = 0.859) at a threshold of −1.8 % (or |1.8|) were valuable too but they were not identified in the multivariable analysis. This multivariable logistic regression leads that the base-apex gradient of mid-wall strain as the independent parameter that improves the positive diagnosis of LVNC (cut-off = −0.18; OR = 0.76, CI 95 % [0.65; 0.90], p = 0.001). These calculations allowed the scientific demonstration of the potential value, not for its own, but in association with previously described approach, of the longitudinal strain. Nevertheless, our message is not to measure these gradient but to look at the bull eyes and the repartition of the longitudinal strain values. Compacted segments at the base have depressed strain values and non-compacted segments (at the apex) have more preserved longitudinal strain values. That is very simple to look for as displayed in Fig. 2.

Limitations

The course of the disease seems different in LVNC and DCM, therefore the age, the sizes of cavities are different. We decided to report about the whole cohort of LVNC and of DCM analyzed during the same period of time with the same bi-modality approach because, we strongly believe that the characteristics of the LVNC might differ from the DCM patients. The diagnosis of LVNC is difficult is case of dilated dysfunctioning LV but is also very difficult in case of preserved LV ejection fraction as it has been reported in athletes for instance [30]. Of course, the populations are limited but LVNC is a rare cardiomyopathy [31].

Conclusion

Myocardial deformations appear informative in distinguishing idiopathic DCM from LVNC. There is a base-apex gradient that identifies significantly more marked apical deformations in LVNC. This functional approach could help diagnose particularly difficult cases according to anatomical appearance.

Acknowledgments Marie Guinoiseau, Valérie Le Moal, Patricia Bouillet for their skillful assistance.

Funding This study was funded by our research lab on its own credits.

Compliance with ethical standards

Conflict of interest Fanny Tarando and Damien Coisne declares that they has no conflict of interest, like the other except the senior author who received a grand from General Electric healthcare for another project.

Ethical approval All procedures performed in studies involving human participants were in accordance with the ethical standards of the institutional and/or national research committee and with the 1964 Helsinki declaration and its later amendments or comparable ethical standards.

Informed consent Informed consent was obtained from all individual participants included in the study, the study was accepted by the regional ethical committee (ethic committee authorization 35RC14-9767).

Appendix

See Tables 7 and 8.

Table 7 Comparison of the characteristics of the LVNC in the cohort of derivation (Rennes) versus the cohort of validation (Poitiers)

Variable	Rennes (n = 48)	Poitiers (n = 41)	P
Gender	48	41	p = 0.5376 (K)
Women	19 (39.6%)	18 (43.9%)	
Men	29 (60.4%)	23 (56.1%)	
Age	47	41	p = 0.1564 (S)
	50.3 ± 17.2	45 ± 17.6	
	(17; 39; 53; 63; 82)	(13; 32; 44; 60; 80)	
Weight (kg)	48	41	p = 0.4691 (S)
	71.4 ± 15	69.2 ± 13.7	
	(50; 59; 69; 81.5; 111)	(38; 60; 66; 80; 95)	
Hight (cm)	48	41	p = 0.3308 (S)
	169.3 ± 9.3	167.4 ± 9.2	
	(154; 160; 168; 176.5; 186)	(149; 162; 168; 174; 187)	
Body Mass Index	48	41	p = 0.7437 (S)
	24.9 ± 4.6	24.6 ± 3.8	
	(18.2; 21.8; 24.5; 26.8; 41.6)	(16.9; 21.6; 24.2; 27.3; 32.8)	
Systolic arterial pressure	39	19	p = 0.4532 (S)
(mm Hg)	125.2 ± 16.6	121.4 ± 19.7	
	(82; 110; 125; 140; 165)	(86; 104; 126; 137; 163)	
Diastolic arterial pressure	39	19	p = 0.4880 (S)
(mm Hg)	74.4 ± 11.2	72.1 ± 13.4	
	(47; 70; 70; 80; 105)	(48; 60; 74; 84; 91)	
IVS thickness (mm)	47	38	p = 0.7104 (S)
	8.8 ± 2.4	9 ± 2	
	(4.7; 7.5; 8.2; 10; 17.9)	(4.4; 7.7; 9; 10; 14.2)	
LVeDD (mm)	47	38	p = 0.5312 (S)
	58 ± 11.1	56.6 ± 9.1	
	(34.3; 50.5; 56; 64.4; 87.9)	(34.5; 52.1; 55.3; 63.5; 72.1)	
Index LVeDD (mm/m²)	44	38	p = 0.8792 (S)
	32.3 ± 6.8	32.5 ± 5.4	
	(18.1; 27.2; 32.3; 35.6; 57.1)	(22.4; 29.1; 31.7; 33.7; 46)	
PW thickness (mm)	47	38	p = 0.1140 (S)
	8.7 ± 2.4	9.4 ± 1.6	
	(5.1; 6.7; 8.2; 10.3; 15.3)	(6.2; 8.4; 9.1; 10; 13.1)	
LVeSD (mm)	47	38	p = 0.0132 (S)
	49.1 ± 12.7	42.2 ± 12	
	(27.6; 39; 47.8; 59.1; 86)	(23.8; 32.6; 39.6; 52.8; 65.3)	
Indexed LVeSDD (mm/m²)	47	39	p = 0.0230 (S)
	27.5 ± 7.7	23.6 ± 8	
	(15.7; 20.5; 28.1; 31.2; 55.8)	(0; 18.4; 21.4; 29.3; 41.2)	
Indexed LA volume (ml/m²)	44	14	p = 0.8841 (S)
	32.2 ± 13	31.7 ± 10.6	
	(15.3; 24.1; 29.4; 35.3; 75)	(14.7; 25.2; 28.5; 41; 51.7)	
Indexed LVeD volume (ml/m²)	45	34	p = 0.0119 (S)
	91.5 ± 43.7	68.7 ± 31.2	
	(23.8; 62.7; 80.1; 102.3; 220.8)	(27.1; 45.9; 60.8; 79.3; 146.3)	
Indexed LVeS volume	48	38	p = 0.0055 (S)
(ml/m²)	59.1 ± 41.8	37.1 ± 25.2	

Table 7 (continued)

Variable	Rennes (n = 48)	Poitiers (n = 41)	P
	(0; 27; 45.8; 72.7; 190.9)	(6.8; 18.3; 27.4; 52.3; 103.5)	
SV Rest (ml)	45	38	p = 0.1156 (S)
	57.9 ± 16.4	52.1 ± 17.2	
	(22.8; 47.4; 54; 68; 105)	(20.8; 38.8; 50.1; 66.3; 90.4)	
LVEF(%)	47	41	p = 0.0046 (S)
	39.6 ± 13.1	48.7 ± 16.1	
	(15; 27; 41; 50; 68)	(23; 33.2; 49.3; 62.5; 75)	
HR	47	37	p = 0.7789 (S)
	68.6 ± 11.3	69.4 ± 13.3	
	(46; 60; 66; 75; 95)	(46; 61.2; 69.6; 76.4; 114.9)	
LVOT VTI (cm)	46	37	p = 0.1148 (S)
	16.5 ± 5.7	18.4 ± 4.3	
	(4.8; 12.8; 16.3; 19.6; 29.2)	(5.7; 16.6; 18.5; 21.9; 25.7)	
Mitral inflow E/A	46	33	p = 0.0186 (S)
	1.2 ± 0.7	1.6 ± 1	
	(0; 0.7; 1; 1.3; 3.7)	(0.6; 0.9; 1.4; 2; 4.5)	
E-dec time (ms)	46	33	p = 0.0409 (S)
	196.8 ± 68.6	169.6 ± 36	
	(72; 151; 182; 244; 354.7)	(75.1; 144.7; 164.2; 201.6; 246.6)	
E/e′ (septal and lateral averaged) (cm/s)	43	13	p = 0.2785 (S)
	11.7 ± 7.9	9 ± 6.6	
	(3.3; 7.2; 9.8; 12.5; 47)	(4.4; 5.4; 6.8; 8.9; 29.2)	
TAPSE (mm)	44	32	p = 0.2944 (S)
	22.4 ± 5	21.2 ± 5.3	
	(10.3; 19; 22.7; 26.1; 30.5)	(6.6; 18.2; 22; 25; 29.3)	
RV s′ (cm/s)	41	30	p = 0.8739 (S)
	11.9 ± 2.7	11.8 ± 3.6	
	(7; 10; 12; 13; 19)	(3.7; 10.2; 11.8; 13.9; 22.1)	
TR Vmax (m/s)	24	20	p = 0.3273 (S)
	3.3 ± 4.4	2.3 ± 0.5	
	(1.1; 2.2; 2.4; 2.7; 24)	(1.7; 1.9; 2.2; 2.6; 3.5)	

Qualitatif Parameters: Effectif (%), test χ^2 (K)

Quantitatif Parameters: Mean ± standart deviation (min; Q1; médiane; Q3; max), test Student (S)

LVeDD left ventricular end-diastolic diameter, *LVeSD* left ventricular end-systolic diaeter, *LA* left atrial, *SV* stroke volume, *HR* heart rate, *LVOT VTI* velocity time integral recorded in the left entricular outflow tract; *E-dec time* mitral inflow E wave deceleration time, *TAPSE* tricuspid annular plan systolic excursion, *TR* tricuspid regurgitation, *RV* right ventricle

Table 8 Comparison of the strain in LVNC patients in the derivation cohort (Rennes) and the validation cohort (Poitiers)

Variable	Rennes (n = 48)	Poitiers (n = 41)	P
Apical Strain EPI	43	40	p = 0.0404 (S)
	−11.5 ± 5.3	−14.2 ± 6.8	
	(−21; −14.2; −12; −8.6; 0)	(−26.8; −19.5; −15.3; −9.9; −0.5)	
Median Strain EPI	43	40	p = 0.0506 (S)
	−11 ± 5	−13.4 ± 5.9	
	(−22.5; −14.5; −11.2; −7.5; 0.8)	(−23; −17.8; −14.2; −9.1; −1.6)	
Basal Strain EPI	43	40	p = 0.0896 (S)
	−9.4 ± 5	−11.4 ± 5.3	
	(−20.3; −13.3; −10.2; −6.3; 1.3)	(−19.3; −16.1; −11.8; −7.3; −1.4)	
Base-Apex Gradient EPI	48	41	p = 0.2871 (S)
	−1.8 ± 3.5	−2.8 ± 5	
	(−13.5; −3.6; −0.9; 0; 7.2)	(−13.6; −5.2; −2.5; −0.1; 14.5)	
Apico-lateral/septal Gradient EPI	48	41	p = 0.0128 (S)
	−1.8 ± 4.4	−5 ± 7.2	
	(−16; −4.3; −0.9; 1.6; 6.2)	(−18.5; −8.1; −4; 0; 6.6)	
GLS EPI	48	37	p = 0.0014 (S)
	−10.2 ± 6.1	−15.4 ± 8.4	
	(−21.5; −13.8; −11.8; −5.5; 0)	(−29.9; −22.1; −17.8; −12.1; 2.4)	
Base –Apex Gradient 4 ch EPI	48	41	p = 0.7912 (S)
	−2 ± 5.6	−2.4 ± 8.9	
	(−20; −4.8; −1; 1.8; 11)	(−24.9; −7.1; −3.2; 2.2; 21.1)	
Apical Strain MID	43	40	p = 0.0780 (S)
	−14.2 ± 6.5	−17.1 ± 8.3	
	(−26.4; −18.2; −14.8; −10.6; −0.4)	(−31.3; −23.8; −18.6; −11.3; −0.8)	
Median Strain MID	43	40	p = 0.0630 (S)
	−12.1 ± 5.6	−14.6 ± 6.3	
	(−24.7; −16; −12.2; −8.3; 0.7)	(−24.9; −19.6; −15.4; −10.1; −1.5)	
Basal Strain MID	43	40	p = 0.0714 (S)
	−10.2 ± 5.3	−12.3 ± 5.4	
	(−21.5; −14.3; −10.8; −6.7; 1.5)	(−20.9; −17.3; −12.5; −8; −1.8)	
Base-Apex Gradient MID	48	41	p = 0.3227 (S)
	−3.6 ± 4.2	−4.7 ± 6	
	(−15.3; −6.1; −2.8; −0.4; 7.8)	(−19; −7.5; −4; −1.3; 15)	
	(−22; −13.5; −10.8; −3.5; 4.5)	(−22.7; −14.6; −10.5; −5.8; 4)	
Apico-lateral/septal Gradient MID	48	41	p = 0.0106 (S)
	−2.8 ± 4.2	−6.1 ± 7.6	
	(−14.5; −5.2; −2.4; 0; 6.5)	(−19.2; −10.7; −5.6; 0; 6.6)	
GLS MID	48	37	p = 0.0018 (S)
	−12.5 ± 7.6	−18.8 ± 10.2	
	(−26; −17.5; −14; −4.8; 0)	(−34.6; −25.4; −20.3; −14.1; 2.3)	
Base-Apex Gradient 4 ch MID	48	41	p = 0.5108 (S)
	−3.4 ± 6.4	−4.6 ± 10.4	
	(−20; −7; −3.3; 0.3; 11)	(−34.6; −10.3; −4.6; 2; 22)	
Apical Strain ENDO	43	40	p = 0.1767 (S)
	−18.5 ± 8.7	−21.4 ± 10.7	
	(−33.6; −25.8; −19; −13.2; −0.8)	(−37.7; −30.4; −23.1; −13.5; −1.2)	
Median Strain ENDO	43	40	p = 0.0810 (S)

Table 8 (continued)

Variable	Rennes (n = 48)	Poitiers (n = 41)	P
	−13.5 ± 6.2	−16 ± 6.7	
	(−27; −18; −13.8; −9.3; 0.7)	(−27.1; −20.8; −17.3; −11.3; −1.3)	
Basal Strain ENDO	43	40	p = 0.0579 (S)
	−11 ± 5.5	−13.3 ± 5.5	
	(−22.5; −15.2; −11.3; −7.2; 1.5)	(−22.9; −17.9; −13.8; −9.4; −2.3)	
Base-Apex Gradient ENDO	48	41	p = 0.4321 (S)
	−6.7 ± 6	−7.9 ± 8	
	(−18.1; −10.7; −5.7; −2; 8.7)	(−28.6; −14; −6.9; −3.7; 15)	
Apico-lateral/septal Gradient ENDO	48	41	p = 0.0320 (S)
	−5 ± 4.2	−8 ± 8.6	
	(−12.8; −7.7; −5.1; −0.8; 2)	(−25.5; −14.8; −9; −0.4; 8.7)	
GLS ENDO	48	37	p = 0.0059 (S)
	−16.8 ± 9.9	−23.9 ± 13.1	
	(−33.5; −24; −19.3; −8.5; 0)	(−48; −32.2; −27.2; −16.4; 2)	
Base-Apex Gradient 4 ch ENDO	48	41	p = 0.5047 (S)
	−6.8 ± 7.4	−8.3 ± 13.2	
	(−22.5; −12.3; −5.3; −0.8; 7)	(−48; −15.4; −8; 0; 22.8)	

Quantitative parameters: Mean ± standart deviation (min; Q1; médiane; Q3; max), test Student (S)

EPI epicardic, *Mid* mid layer, *ENDO* endocardic, *GLS* global longitudinal strain, *4 ch* 4 chamber view

References

1. Jenni R, Oechslin E, Schneider J, Attenhofer Jost C, Kaufmann PA (2001) Echocardiographic and pathoanatomical characteristics of isolated left ventricular non-compaction: a step towards classification as a distinct cardiomyopathy. Heart 86:666–671
2. Arbustini E, Weidemann F, Hall JL (2014) Left ventricular noncompaction: a distinct cardiomyopathy or a trait shared by different cardiac diseases? J Am Coll Cardiol 64:1840–1850
3. Stollberger C, Finsterer J, Blazek G (2002) Left ventricular hypertrabeculation/noncompaction and association with additional cardiac abnormalities and neuromuscular disorders. Am J Cardiol 90:899–902
4. Hussein A, Karimianpour A, Collier P, Krasuski RA (2015) Isolated noncompaction of the left ventricle in adults. J Am Coll Cardiol 66:578–585
5. Pinto FJ (2015) When and how to agree in disagreeing on the diagnosis of noncompaction by echocardiography? JACC Cardiovasc Imaging 8:1258–1259
6. Stollberger C, Gerecke B, Engberding R, Grabner B, Wandaller C, Finsterer J, Gietzelt M, Balzereit A (2015) Interobserver agreement of the echocardiographic diagnosis of lv hypertrabeculation/noncompaction. JACC Cardiovasc Imaging 8:1252–1257
7. Petersen SE (2015) Left Ventricular noncompaction: a clinically useful diagnostic label? JACC Cardiovasc Imaging 8:947–948
8. Chin TK, Perloff JK, Williams RG, Jue K, Mohrmann R (1990) Isolated noncompaction of left ventricular myocardium. A study of eight cases. Circulation 82:507–513
9. Ritter M, Oechslin E, Sutsch G, Attenhofer C, Schneider J, Jenni R (1997) Isolated noncompaction of the myocardium in adults. Mayo Clin Proc 72:26–31
10. Petersen SE, Selvanayagam JB, Wiesmann F, Robson MD, Francis JM, Anderson RH, Watkins H, Neubauer S (2005) Left ventricular non-compaction: insights from cardiovascular magnetic resonance imaging. J Am Coll Cardiol 46:101–105
11. Jacquier A, Thuny F, Jop B, Giorgi R, Cohen F, Gaubert JY, Vidal V, Bartoli JM, Habib G, Moulin G (2010) Measurement of trabeculated left ventricular mass using cardiac magnetic resonance imaging in the diagnosis of left ventricular non-compaction. Eur Heart J 31:1098–1104
12. Oechslin EN, Attenhofer Jost CH, Rojas JR, Kaufmann PA, Jenni R (2000) Long-term follow-up of 34 adults with isolated left ventricular noncompaction: a distinct cardiomyopathy with poor prognosis. J Am Coll Cardiol 36:493–500
13. Murphy RT, Thaman R, Blanes JG, Ward D, Sevdalis E, Papra E, Kiotsekoglou A, Tome MT, Pellerin D, McKenna WJ et al (2005) Natural history and familial characteristics of isolated left ventricular non-compaction. Eur Heart J 26:187–192
14. Kohli SK, Pantazis AA, Shah JS, Adeyemi B, Jackson G, McKenna WJ, Sharma S, Elliott PM (2008) Diagnosis of left-ventricular non-compaction in patients with left-ventricular systolic dysfunction: time for a reappraisal of diagnostic criteria? Eur Heart J 29:89–95
15. Sengupta PP, Mohan JC, Mehta V, Jain V, Arora R, Pandian NG, Khandheria BK (2004) Comparison of echocardiographic features of noncompaction of the left ventricle in adults versus idiopathic dilated cardiomyopathy in adults. Am J Cardiol 94:389–391
16. Niemann M, Liu D, Hu K, Cikes M, Beer M, Herrmann S, Gaudron PD, Hillenbrand H, Voelker W, Ertl G et al (2012) Echocardiographic quantification of regional deformation helps to distinguish isolated left ventricular non-compaction from dilated cardiomyopathy. Eur J Heart Fail 14:155–161
17. Bellavia D, Michelena HI, Martinez M, Pellikka PA, Bruce CJ, Connolly HM, Villarraga HR, Veress G, Oh JK, Miller FA (2010) Speckle myocardial imaging modalities for early detection of myocardial impairment in isolated left ventricular non-compaction. Heart 96:440–447
18. Elliott P, Andersson B, Arbustini E, Bilinska Z, Cecchi F, Charron P, Dubourg O, Kuhl U, Maisch B, McKenna WJ et al (2008) Classification of the cardiomyopathies: a position statement from the

European Society Of Cardiology Working Group on Myocardial and Pericardial Diseases. Eur Heart J 29:270–276
19. Cosyns, B., Garbi, M., Separovic, J., Pasquet, A., Lancellotti, P.; Education Committee of the European Association of Cardiovascular Imaging, A. (2013). Update of the echocardiography core syllabus of the European Association of Cardiovascular Imaging (EACVI). Eur Heart J Cardiovasc Imaging 14, 837–839.
20. Lang RM, Badano LP, Mor-Avi V, Afilalo J, Armstrong A, Ernande L, Flachskampf FA, Foster E, Goldstein SA, Kuznetsova T et al (2015) Recommendations for cardiac chamber quantification by echocardiography in adults: an update from the American Society of Echocardiography and the European Association of Cardiovascular Imaging. Eur Heart J Cardiovasc Imaging 16:233–270
21. DeLong ER, DeLong DM, Clarke-Pearson DL (1988) Comparing the areas under two or more correlated receiver operating characteristic curves: a nonparametric approach. Biometrics 44:837–845
22. Sengelov M, Jorgensen PG, Jensen JS, Bruun NE, Olsen FJ, Fritz-Hansen T, Nochioka K, Biering-Sorensen T (2015) Global longitudinal strain is a superior predictor of all-cause mortality in heart failure with reduced ejection fraction. JACC Cardiovasc Imaging 8:1351–1359
23. Phelan D, Collier P, Thavendiranathan P, Popovic ZB, Hanna M, Plana JC, Marwick TH, Thomas JD (2012) Relative apical sparing of longitudinal strain using two-dimensional speckle-tracking echocardiography is both sensitive and specific for the diagnosis of cardiac amyloidosis. Heart 98:1442–1448
24. Vatta M, Mohapatra B, Jimenez S, Sanchez X, Faulkner G, Perles Z, Sinagra G, Lin JH, Vu TM, Zhou Q et al (2003) Mutations in Cypher/ZASP in patients with dilated cardiomyopathy and left ventricular non-compaction. J Am Coll Cardiol 42:2014–2027
25. Schweizer PA, Schroter J, Greiner S, Haas J, Yampolsky P, Mereles D, Buss SJ, Seyler C, Bruehl C, Draguhn A et al (2014) The symptom complex of familial sinus node dysfunction and myocardial noncompaction is associated with mutations in the HCN4 channel. J Am Coll Cardiol 64:757–767
26. Milano A, Vermeer AM, Lodder EM, Barc J, Verkerk AO, Postma AV, van der Bilt IA, Baars MJ, van Haelst PL, Caliskan K et al (2014) HCN4 mutations in multiple families with bradycardia and left ventricular noncompaction cardiomyopathy. J Am Coll Cardiol 64:745–756
27. Towbin JA, Lorts A, Jefferies JL (2015) Left ventricular noncompaction cardiomyopathy. Lancet 386:813–825
28. Captur G, Nihoyannopoulos P (2010) Left ventricular non-compaction: genetic heterogeneity, diagnosis and clinical course. Int J Cardiol 140:145–153
29. Choudhary P, Hsu CJ, Grieve S, Smillie C, Singarayar S, Semsarian C, Richmond D, Muthurangu V, Celermajer DS, Puranik R (2015) Improving the diagnosis of LV non-compaction with cardiac magnetic resonance imaging. Int J Cardiol 181:430–436
30. Caselli S, Ferreira D, Kanawati E, Di Paolo F, Pisicchio C, Attenhofer Jost C, Spataro A, Jenni R, Pelliccia A (2016) Prominent left ventricular trabeculations in competitive athletes: A proposal for risk stratification and management. Int J Cardiol 223:590–595
31. Habib G, Charron P, Eicher JC, Giorgi R, Donal E, Laperche T, Boulmier D, Pascal C, Logeart D, Jondeau G et al (2011) Isolated left ventricular non-compaction in adults: clinical and echocardiographic features in 105 patients. Results from a French registry. Eur J Heart Fail 13:177–185